

~~NASA CR-130064~~

PHOTOIONIZATION MEASUREMENT STUDY

by

Guido Sandri and Alexander Klimas

Aeronautical Research Associates of Princeton, Inc.
50 Washington Road, Princeton, New Jersey 08540

February 1972

(NASA-CR-130064) PHOTOIONIZATION MEASUREMENT STUDY Final Report, 26 Feb. 1971 - 25 Feb. 1972 G. Sandri (Aeronautical Research Associates of Princeton) Feb. 1972 41 p	N72-32786
CSCL 03B G3/29	Unclas 43415

Final Report
for period
February 26, 1971 - February 25, 1972



Prepared for
GODDARD SPACE FLIGHT CENTER
Greenbelt, Maryland 20771

1. Report No.	2. Government Accession No.	3. Recipient's Catalog No.	
4. Title and Subtitle Photoionization Measurement Study		5. Report Date February 1972	
		6. Performing Organization Code	
7. Author(s) Guido Sandri		8. Performing Organization Report No.	
9. Performing Organization Name and Address Aeronautical Research Associates of Princeton, Inc. 50 Washington Road Princeton, New Jersey 08540		10. Work Unit No.	
		11. Contract or Grant No. NAS5-11402	
12. Sponsoring Agency Name and Address NASA, Goddard Space Flight Center Greenbelt, Maryland 20771 Dr. E. A. Boldt, Technical Monitor		13. Type of Report and Period Covered Final Report 2/26/71 - 2/25/72	
		14. Sponsoring Agency Code	
15. Supplementary Notes			
16. Abstract We have carried out an analysis of a gas window photoionization device for studying cosmic x-rays in the region 20 eV to 1 KeV. The detecting element is an argon proportional counter whose window is a two-dimensional supersonic gas jet. Spectroscopic features of the incoming radiation can be determined by the choice of gas forming the jet (as well as by the fluid dynamic parameters of the flow). The choice of gas can be made from pure substances and/or compounds with Z between 1 and 10. The counter walls can be prepared for selective analysis of the extreme ultraviolet radiation.			
17. Key Words (Selected by Author(s)) Proportional Counter Low-energy x-ray Detector Photoionization Device		18. Distribution Statement	
19. Security Classif. (of this report) Unclassified	20. Security Classif. (of this page) Unclassified	21. No. of Pages 40	22. Price* \$4.25

*For sale by the Clearinghouse for Federal Scientific and Technical Information, Springfield, Virginia 22151.

TABLE OF CONTENTS

<u>SECTION</u>		<u>PAGE</u>
	Preface	iii
	List of Illustrations.....	v
	List of Tables.....	vi
I	Introduction.....	1
II	Argon Flow Rate.....	4
	A. Continuum Calculations.....	6
	B. Free Molecular Flow.....	10
	C. Intermediate Flow Regimes.....	13
III	Helium Jet.....	19
IV	Helium-Argon Interaction.....	26
V	Conclusions and Recommendations.....	31
	References.....	32

PREFACE

A problem of growing importance in x-ray astronomy is the detection of low-energy x-rays (below 1 KeV). To obtain information on low-energy cosmic rays, it is important to minimize the role of the window on the counter.

We have carried out an analysis of a gas window photoionization device for studying cosmic x-rays in the region 20 eV to 1 KeV. The detecting element is an argon proportional counter whose window is a two-dimensional supersonic gas jet. Spectroscopic features of the incoming radiation can be determined by the choice of gas forming the jet (as well as by the fluid dynamic parameters of the flow). The choice of gas can be made from pure substances and/or compounds with Z between 1 and 10. The counter walls can be prepared for selective analysis of the extreme ultraviolet radiation.

A preliminary study of the fluid dynamic requirements had shown that the relevant parameters (mass flow, pressure, and Mach number) could be chosen for satisfactory counter performance. This preliminary analysis was largely based on the assumption that the argon flow through the porous wall could be treated with fluid equations. In this report, we incorporate the fluid analysis. In addition, we study the case when the mean free path of the argon gas is comparable to the radius of a typical hole in the porous window of the counter and, thus, kinetic theory is needed. This case is essential for the practical operation of the counter. The broad feasibility conclusion has not changed.

Some of the advantages offered by the gas window counter, as contrasted to more standard detectors, are:

1. Extension of efficient low-energy x-ray observations below presently accessible energies.
2. Multicolor or digital spectrometry made possible by the availability of pure element filters (H, He, Ni, O, Ne). Methane and Freon are also possible suitable filters.

This counter can be uniquely applied to the observation of a number of radiation problems of current interest; in particular, low-energy diffuse x-ray background, soft x-rays (including O and Ne line emission) from nearby stars, soft x-rays from the solar wind which are expected to be predominantly at about 100 eV, recombination radiation of low-energy cosmic ray nuclei, and interstellar absorption of x-ray fluxes from distant objects.

In brief summary, our study shows that the fluid dynamic features that enter the performance of the device do not present fundamental difficulties. The theoretical analysis should be implemented by experiments to obtain a realistic optimization of all the parameters. We can summarize the design characteristics that are recommended as follows:

- total open area = 10 cm^2
- argon pressure = 1 mm Hg
- typical hole diameter = .01 cm
- porous wall thickness = .005 cm
- number of holes $\approx 10^5$
- helium nozzle diameter $\approx 7.5 \text{ cm}$
- helium jet Mach number ≈ 7.00
- throat radius $\approx 1.00 \text{ cm}$
- throat opening $\approx .1 \text{ cm}$
- pressure in the helium tank $\approx 100 \text{ mm Hg}$.

LIST OF ILLUSTRATIONS

- Figure 1. Schematic of the Low-energy X-ray Counter, page 2 .
- Figure 2. Argon Flow Geometry, page 5 .
2a. Suggested Values of the Geometric Parameters
2b. Geometry for Kinetic Theory Analysis of the
Motion of an Outflowing Argon Molecule
- Figure 3. The Mass of Argon Gas Crossing the Counter's Window
per Second as a Function of Number of Holes, page 17.
- Figure 4. Helium Nozzle Geometry and Fluid Dynamic Properties
with Suggested Parameter Values for Counter Operation,
page 20.

LIST OF TABLES

Table 1. Comparison of Calculations for Intermediate Regimes,
page 14.

Table 2. Helium Jet Parameters, page 25.

I. INTRODUCTION

The basic idea suggested by Dr. Peter Serlemitsos of the Goddard Space Flight Center is illustrated in Figure 1. The usual thin window is replaced by a porous material that will transmit low-energy x-rays. The argon that escapes through the window is blown away by a helium jet. Argon is supplied to the chamber through a porous base so that a pressure of about 1 mm Hg is maintained in the chamber.

Three basic problems must be considered to ascertain the proper operation of the counter:

1. The flow of argon through the porous window. The quantity to be determined here is the mass flow rate of argon through a suitable porous wall.
2. The flow field of the helium jet. In particular, the wall pressure and mass flux of helium gas.
3. The helium-argon interaction. In particular, the blowing parameter whose "critical" value cannot be exceeded if the argon gas is to be swept clean from the porous window.

The counter could be flown by means of a rocket. The exposure time would then be approximately 2 minutes. An important figure of merit, then, is the total mass of He that must be carried for continuous operation during this time. The helium mass per second can be bracketed with reasonable certainty by considering the two extremes, calculations of the argon flow rate given by the continuum (hydrodynamic) equations and the free molecule effusion. For the helium mass per second, we find

$$Q_{\text{He}}(\text{cont}) \approx 1 \text{ gm/sec} \quad (1.1)$$

$$Q_{\text{He}}(\text{eff}) \approx 5 \text{ gm/sec} \quad (1.2)$$

from which we conclude that the total helium mass needed is bracketed by

$$120 \text{ gm} < \text{Mass}(\text{he}) < 600 \text{ gm} \quad (1.3)$$

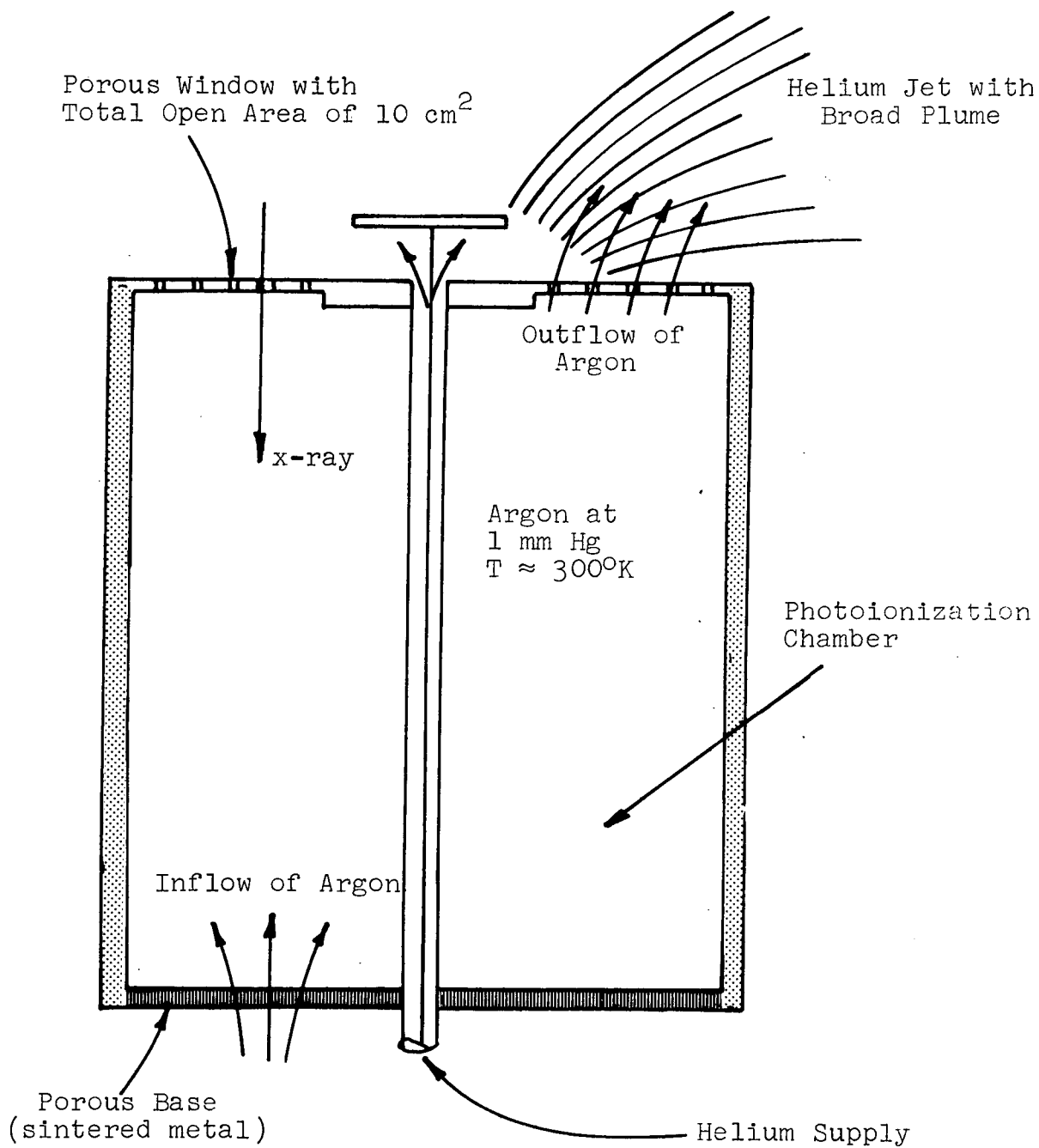


Figure 1. Schematic of the Low-energy X-ray Counter

Even the conservative amount of 600 gm does not seem prohibitive. The pressure in the helium tank is determined to be about 1 atmosphere. The argon mass needed is found to be about 1/10th of the helium mass. The Mach number of the helium jet is found to be between 7 and 10. A typical hole radius, window thickness, and argon gas mean free path are approximately .5 mil (1 mil = 10^{-3} in. = 2.54×10^{-3} cm).

Optimization of the parameters is not feasible without experimentation in view of the considerations that follow.

The flow rate of argon through the porous windows has been determined theoretically only for some specific values of the basic parameters, λ/l , l/D and f , where

- λ = mean free path of the argon gas
- l = height of a typical hole in the porous window
- D = diameter of a typical hole in the porous window
- f = accommodation coefficient of the argon gas to the wall of the hole = fraction of argon molecules that hit the hole wall and are diffusely reflected at the wall temperature.

Additional theoretical uncertainties are due to hole shape and to the wall pressure and temperature gradient (thermal creep) across the porous window generated by the cold hypersonic helium flow.

Experiments on flow through pipes and orifices have been carried out only with a few materials and gases. Furthermore, the experimental results available are also restricted to special values of λ/l and l/D .

The hypersonic nozzle for the helium jet will have a very narrow throat. It is not feasible to determine the operation conditions of such a throat on purely theoretical grounds.

The skin friction coefficient C_f that characterizes the blowing parameter is an empirical coefficient which is known only under rather special conditions.

II. ARGON FLOW RATE

A quantity of major importance for the understanding of the counter's operation is the mass flow rate of the argon gas through the porous window. For proper counter operation, it is essential to minimize the argon flow rate because of two separate conditions:

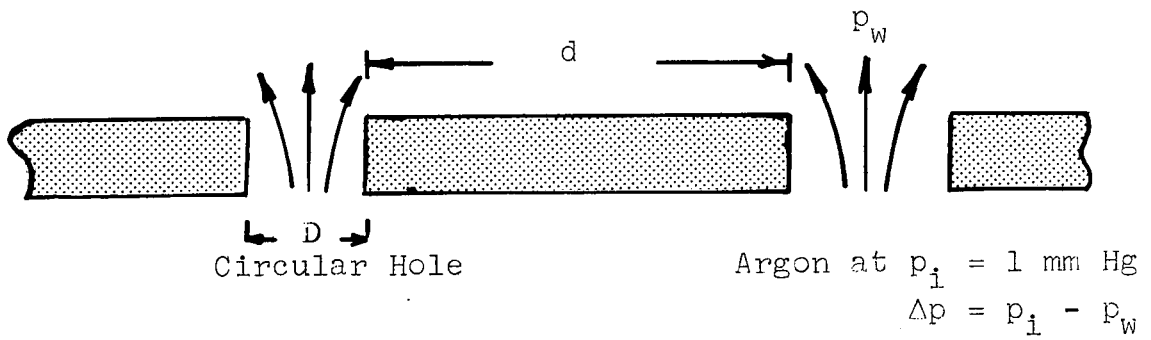
1. The total mass of argon needed during a two-minute exposure of the counter should not be prohibitive.
2. The blowing parameter discussed in Section IV cannot exceed its critical value b_{crit} ; otherwise, there is argon gas in front of the porous window.

Below, we show that the first requirement is easily satisfied while the second is not. In this chapter, we first calculate the argon flow rate in two extreme regimes: continuous (or fluid) flow and free molecular (or rarefied) flow. We then summarize the theoretical analyses of intermediate regimes. The two extreme calculations differ by a factor of two; thus,

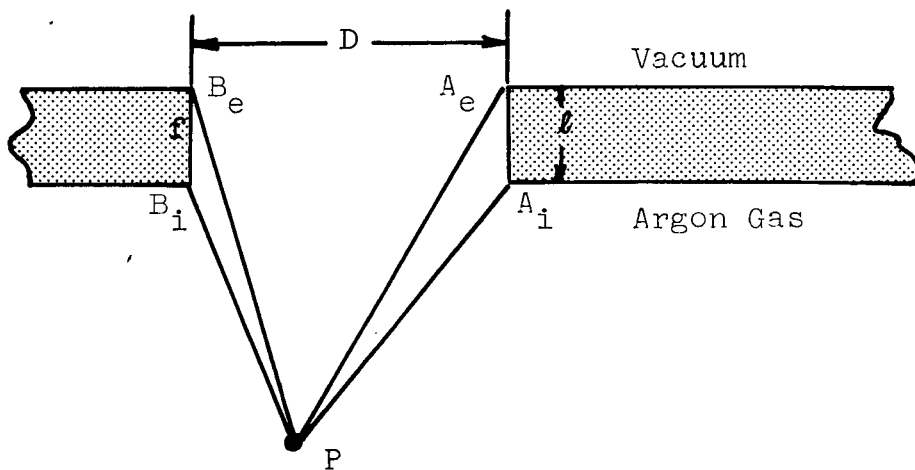
$$Q_{Ar}(eff) \approx 2Q_{Ar}(cont) \quad (2.1)$$

Intermediate flow regimes could conceivably give results in excess to the upper value or below the lower value, as shown by some intermediate calculations. In our opinion, the ultimate minimization of the argon flow can be obtained only experimentally since several factors may provide a final adjustment. For example, circular holes probably yield maximal flow rate so that slit-shaped or star-shaped holes may be more desirable, especially if properly accommodating window material and gas are found. Also, the wall pressure and the thermal gradient induced by the helium jet may diminish somewhat the argon flow.

In Figure 2, we show the geometry of the argon gas outflow from the photoionization chamber. In Figure 2a, the values of the hole parameters suggested by our theoretical analysis are shown. In Figure 2b, we indicate the geometry for the kinetic



2a. Suggested Values of the Geometric Parameters
 $D \approx .01 \text{ cm} \approx 4 \text{ mil}$, $l \approx .005 \text{ cm} \approx 2 \text{ mil}$,
 $d \approx .03 \text{ cm} \approx 12 \text{ mil}$



2b. Geometry for Kinetic Theory Analysis of the Motion of an Outflowing Argon Molecule

Figure 2. Argon Flow Geometry

theory analysis of the motion of an argon molecule at P . The theoretical uncertainties in the argon flow stem from two opposing mechanisms. Namely, the molecules within the cone A_ePB_e have low density (collisions raise their density) while within the cone $A_iPB_i-A_ePB_e$ the accommodation to the wall is essential (any amount of accommodation reducing the momentum of an escaping molecule). The precise dependence of these two effects on l and D is not available.

A. Continuum Calculations

Now, we suppose that the average hole size in the window is sufficiently small that the argon velocity is very much less than acoustic. Then we can estimate the flow rate for a typical hole with the Hagen-Poiseuille formula for pipe flow. Since this formula corresponds to incompressible, nonturbulent fluid flow, we shall check below that both the Mach and the Reynolds numbers for the flow are small.

Referring to Figure 2 and Reference 1, p. 10, we obtain for the average velocity of the argon gas

$$\bar{u}_{Ar} = \frac{D^2 \Delta p}{32 l \mu} \quad (2.2)$$

The mass flow rate for a single hole is given by

$$Q_{Ar} = \pi \frac{D^2}{4} \rho \bar{u} \quad (2.3)$$

We shall use the Reynolds number based on the hole diameter

$$Re_{Ar} = \frac{\rho \bar{u} D}{\mu} \quad (2.4)$$

where μ is the viscosity of argon. For this quantity, we use the value (Ref. 2)

$$\mu_{Ar} = 2.0 \times 10^{-4} \text{ gm (cm sec)} \quad (2.5)$$

If we consider the external pressure to be zero, we can obtain an upper bound on the argon flow rate. To be specific, we choose

$$\ell = 0.005 \text{ cm} \quad (2.6)$$

$$D = 0.01 \text{ cm} = 2\ell \quad (2.7)$$

It is important to note that the flow rate varies as D^4 so that we can control it by changing the hole size by a small amount.

The pressure change across the hole is

$$\Delta p = 1330 \text{ dynes/cm}^2 \quad (2.8)$$

Thus, the flow velocity of the argon gas is

$$\begin{aligned} \bar{u}_{\text{Ar}} &= \frac{(.01)^2 (1330)}{32(.005)(2.0 \times 10^{-4})} \\ &= 4150 \text{ cm/sec} \end{aligned} \quad (2.9)$$

It is important to maintain a low Mach number M for the argon flow. The thermal speed of the argon molecule is

$$\begin{aligned} a_{\text{Ar}} &= \sqrt{\gamma RT} = \sqrt{\frac{5}{3}(2.07 \times 10^6)300} \\ &= 3.22 \times 10^4 \text{ cm/sec} \end{aligned} \quad (2.10)$$

and therefore

$$M_{\text{Ar}} = \frac{\bar{u}}{a} = 0.129 \quad (2.11)$$

This low value of the Mach number M indicates that the flow is indeed incompressible so that our use of the Hagen-Poiseuille formula is valid.

The mass density of the argon gas is

$$\begin{aligned} \rho_{\text{Ar}} &= \frac{p}{RT} = \frac{1330}{(2.07 \times 10^6)(300)} \\ &= 2.14 \times 10^{-6} \text{ gm/cm}^3 \end{aligned} \quad (2.12)$$

Combining (2.9) and (2.12), we obtain the momentum density

$$\begin{aligned}(\bar{\rho u})_{Ar} &= (2.14 \times 10^{-6})(4150) \\ &= 8.9 \times 10^{-3} \text{ gm/cm}^2/\text{sec}\end{aligned}\quad (2.13)$$

Therefore, the mass loss rate is

$$\begin{aligned}Q_{Ar} &= 3.14 \frac{(.01)^2}{4} (8.9 \times 10^{-3}) \\ &= 7.0 \times 10^{-7} \text{ gm/sec/hole}\end{aligned}\quad (2.14)$$

The Reynolds number defined in (2.4) is

$$Re_{Ar} = \frac{(8.9 \times 10^{-3})(.01)}{2.0 \times 10^{-4}} = 0.445 \quad (2.15)$$

This low value of the Reynolds number indicates that the flow is laminar and is further justification of our use of the Hagen-Poiseuille formulation.

The number of holes needed can be estimated from the requirement that the total open area must be about 10 cm². Thus, since

$$N_{\text{holes}} \cdot \frac{\pi D^2}{4} = 10 \text{ cm}^2 \quad (2.16)$$

we obtain for the number of holes

$$\begin{aligned}N_{\text{holes}} &= \frac{4(10)}{3.14(.01)^2} \\ &= 1.27 \times 10^5\end{aligned}\quad (2.17)$$

The total argon flow is therefore

$$\begin{aligned}Q_{\text{total}} &= (7.0 \times 10^{-7})(1.27 \times 10^5) \\ &= 0.089 \text{ gm/sec}\end{aligned}\quad (2.18)$$

We emphasize that this value is an upper bound for Q when the helium jet is not operating and for a particular hole size.

The average spacing between holes can be estimated from the fact that about 100 cm^2 is available for distributing the holes. Thus, we obtain for the average spacing

$$\begin{aligned} d &= \sqrt{\frac{100}{N_{\text{holes}}}} = \frac{1}{\sqrt{1270}} \\ &= 0.028 \text{ cm} \approx 3D \end{aligned} \quad (2.19)$$

The fact that the hole spacing is of the same order as the hole diameters is a good indication that the analysis of Section IV (which uses results on boundary layers with blowing) is correct. The foregoing results suggest that the window could be made of a woven material. Metal fabric or fiberglass cloth are two possibilities. Another alternative is to evaporate a material with low atomic number onto an ordinary fabric. The window material will probably have to be put on under tension and stiffened to prevent large static deflection and/or flutter. The porous base to meter the inflow of argon could possibly be made out of a sintered metal.

It is of importance to notice that, in spite of the short length of the "pipe" (hole) through which the argon flows, a fully established Poiseuille profile will hold over most of the hole if the fluid analysis is applicable. Thus, referring to Schlichting's calculation of the development of the Poiseuille profile (Ref. 1, p. 147), we have

$$l = \frac{1}{2} D = a \quad (2.20)$$

Therefore, the Schlichting variable is given by

$$s = 100 \frac{\nu}{aU_0} \frac{x}{a} \quad (2.21)$$

where

$$\nu = \frac{\mu}{\rho} = \text{kinematic viscosity of argon} \quad (2.22)$$

From (2.20)

$$\left(\frac{x}{a}\right)_{\text{exit}} = \frac{l}{a} = 1 \quad (2.23)$$

and

$$\begin{aligned} s_{\text{exit}} &= 100 \frac{\mu}{\rho a U_0} = 200 \frac{\mu}{\rho U_0 D} \\ &= 200/\text{Re} = 400 \end{aligned} \quad (2.24)$$

where we took $U_0 \sim \bar{u}$. Since, from Figure 9.14 of Reference 1, the Poiseuille profile is achieved for $s \sim 5$, we see that flow is fully developed for the hole geometry that we have considered over most of the hole length. Thus, if fluid analysis is appropriate, the argon mass flow rate given by Eq. (2.13) is only slightly underestimated.

B. Free Molecular Flow

Since the completion of the preliminary feasibility study for the low-energy proportional counter, Reference 3, it has become clear that commercially available porous windows can be obtained with hole sizes realistically smaller than those envisaged in Reference 1. We conclude, below, that even using a smaller hole diameter, the argon flow rate is not appreciably changed from the estimate of Reference 3. The diameter of a circular hole in the porous window was taken to be (Eq. (2.7))

$$D \approx 10^{-2} \text{ cm} \quad (2.25)$$

At least one decade can be gained for this figure of merit, according to a number of commercial samples. It becomes important under these conditions to find out if free molecular effects can swamp the fluid analysis given in Reference 3. The standard sufficient criterion for the validity of fluid analysis is that the mean free path be small compared to the characteristic dimensions of the system (D , in our case).

We utilize Jeans' formula, Reference 4, for the average mean free path in a hard sphere gas

$$\lambda_{Ar} = (1.3)[\sqrt{2}\pi n\sigma^2]^{-1} \quad (2.26)$$

where

n = number density of the argon gas

σ = diameter of an argon molecule

and where the factor of 1.3 yields the correction due to persistence of velocities. We show below that the average molecular mean free path is just smaller than the diameter of the hole. We use the following fluid conditions for the argon gas in the photoionization chamber

$$\begin{aligned} p_1 &= \text{internal argon pressure} \\ &= 1 \text{ mm Hg} \end{aligned} \quad (2.27)$$

$$\begin{aligned} T &= \text{approximate absolute temperature} \\ &\quad \text{of the operating counter} \\ &\approx 300^\circ\text{K} \end{aligned} \quad (2.28)$$

and the following atomic parameters

$$\begin{aligned} m &= \text{mass of an argon atom} \\ &= 6.63 \times 10^{-23} \text{ gm} \end{aligned} \quad (2.29)$$

$$\sigma = 3.64 \times 10^{-8} \text{ cm} \quad (2.30)$$

We then obtain for the argon mass and number densities

$$\begin{aligned} \rho_{Ar} &= \text{mass density of the argon within} \\ &\quad \text{the chamber} \\ &= 2.14 \times 10^{-6} \text{ gm cm}^{-3} \end{aligned} \quad (2.31)$$

$$n = .3 \times 10^{17} \text{ cm}^{-3} \quad (2.32)$$

Equation (2.31) is equivalent to (2.12). The resulting average mean free path is $.56 \times 10^{-2}$ cm when the persistence-of-velocities effect is neglected and

$$\lambda \approx .73 \times 10^{-2} \text{ cm} \quad (2.33)$$

when the complete formula (2.32) is utilized. We have used a recent analysis (Ref. 5) of the noble gases' kinetic properties

to check that substantial variations in the temperature do not affect our conclusions. In particular, the diameter given for argon is adequate in the regime considered here.

In view of the rather large λ , we shall compare the results of the Hagen-Poiseuille analysis (fluid flow) with the results of pure effusion (free molecular flow) and show that, in the gas regime of interest for our study, the two types of flows yield comparable flow rates for the argon gas - effusion yielding a higher rate especially for smaller holes.

The Hagen-Poiseuille flow yields, for the argon escape rate, from (2.13)

$$\rho \bar{u} = \rho \frac{D^2 \Delta p}{32 \ell \mu} \approx 8.9 \times 10^{-3} \text{ gr/cm}^2/\text{sec} \quad (2.34)$$

where \bar{u} is the macroscopic velocity. (One can see in the formula the dependence on hole diameter.) The standard kinetic theory result for effusion is (Ref. 4, p. 59)

$$\frac{1}{4} \rho \bar{c} = \rho \sqrt{\frac{kT}{2\pi m}} \quad (2.35)$$

where \bar{c} is the mean molecular velocity at the orifice and T is the absolute temperature inside the chamber. Using the numerical values for ρ , T and m given above, we find

$$\frac{1}{4} \rho \bar{c} \approx 2.1 \times 10^{-2} \text{ gm/cm}^2/\text{sec} \quad (2.36)$$

Thus, for the "larger" holes, viscosity damps the escape of argon. On the other hand, the finer porous walls available commercially may provide improved overall conditions, for example, for the interaction with the helium jet.

The value (2.33) for the mean free path can be confirmed by two separate order-of-magnitude estimates. We first use the relation among Reynolds, Mach and Knudsen numbers (for the argon gas). We have

$$\text{Re} = \frac{\rho \bar{u} D}{(nkT)(\lambda/v_{th})} \quad (2.37)$$

$$v_{th}^2 = 3 \frac{kT}{m} \quad (2.38)$$

Then

$$\text{Re} = 3 \left(\frac{\bar{u}}{v_{th}} \right) \frac{D}{\lambda} = 3M \frac{D}{\lambda} \quad (2.39)$$

Using (2.31) and (2.15)

$$\lambda \sim \frac{.39}{.4} D \sim D \quad (2.40)$$

We also use the kinetic theory relation for gas viscosity

$$\mu \approx \tau p = \frac{\lambda}{v_{th}} p \quad (2.41)$$

Therefore

$$\begin{aligned} \lambda &= \frac{\mu v_{th}}{p} = \frac{(2 \times 10^{-4}) \times (3 \times 10^4)}{1.3 \times 10^3} \\ &\approx .4 \times 10^{-2} \approx D/2 \end{aligned} \quad (2.42)$$

The approximate values (2.40) and (2.42) are full confirmation that the mean free path value (2.33) is compatible with the fluid and kinetic parameters used.

C. Intermediate Flow Regimes

In the two previous subsections, we have discussed two regimes that are likely to bracket the argon flow rate and, therefore, all the other parameters of the gas window counter. A full analysis of the intermediate regimes is not available, but some of the important results obtained theoretically (which we summarize in the following table using the notation of Section I) yield valuable indications. (Remember that f is the

fraction of argon molecules that hit the hole wall and are reflected at the wall temperature.)

	$K = \lambda/D$	ℓ/D	f
1. Hagen-Poiseuille	0	∞	1
2. Kennard	∞	arbitrary	-
3. Rotenberg-Weitzner	$O(1/K)$ near-free mol.	0	-
4. Sone-Yamamoto	$O(K^2)$ near continuum	∞	1
5. Cercignani-Sernagiotto	arbitrary	∞	1

Table 1. Comparison of Calculations for Intermediate Regimes

The calculations included in the above table can be found in the following references:

1. H. Schlichting , Ref. 1, p. 10 and ff.
2. E. Kennard, Ref. 6, p. 308.
3. A. Rotenberg and H. Weitzner, Ref. 7.
4. Y. Sone and K. Yamamoto, Ref. 8.
5. C. Cercignani and F. Sernagiotto, Ref. 9. While the broad conclusions of this work are generally accepted, numerical accuracy is in doubt.

Experimental references are found in the works quoted above. Additional experimental information is found in Reference 10.

A number of valuable conclusions can be extracted from these analyses even though a general expression per second for the mass

passing through a hole of the form

$$Q = Q(K, \ell/D, f) = Q[N_{\text{holes}}, \ell/D, f] \quad (2.43)$$

is not available. The equivalence of the two expressions in Eq. (2.43) is shown below (Eq. (2.50)).

1. The Hagen-Poiseuille flow is discussed in Section II.A. This is appropriate to the continuum regime.
2. From Kennard's formula, we find that for $\ell = a = D/2$,

$$Q_{\text{free mol}} = \frac{2}{3} Q_{\text{eff}} \quad (2.44)$$

where we have used the definition

$$Q_{\text{free mol}} = Q(\infty, \ell/D, 1)$$

When Kennard's formulae are used, note that

$$Q_{\text{Kennard}} = \left(\frac{k}{m} T\right) \cdot Q$$

so that in our notation the mass per second crossing the counter's window is ($R = k/m$)

$$Q = \frac{10}{\pi} \frac{20 + 8(\ell/a)}{20 + 19(\ell/a) + 3(\ell/a)^2} \left(\frac{\pi}{2RT}\right)^{1/2} \Delta p \quad (2.45)$$

This result suggests that the effusion value for the argon flow rate is the upper bound.

3. From the work of Rotenberg and Weitzner, we find that (for the regime given in Table 1 above) and for hard sphere interaction,

$$Q = Q_{\text{free mol}} (1 + .145/K) \quad (2.46)$$

Thus, collisional effects enhance the flow rate from the orifice. We call this effect the R-W "trend." This result suggests that the effusion value can be exceeded. Note,

- however, that the R-W geometry is an "orifice" with $\ell \rightarrow 0$.
4. Sone and Yamamoto find that the Cercignani and Sernagiotto values are correct only to $O(K)$ but not to $O(K^2)$. Also, they give an analysis of the thermal creep.
 5. From Cercignani and Sernagiotto, we obtain a map of Q vs. $K = \lambda/D$ whose main characteristic is a minimum in Q for K between .3 and 1 (i.e., in the regime that we are discussing for the counter). We call this effect the C-S "trend." This result suggests that our choice (Eqs. (2.7) and (2.33))

$$D \approx 2\ell, \quad \lambda \approx D \quad (2.47)$$

is close to minimizing the argon flow rate even though the value of Q remains somewhat uncertain.

The basic features of the flow rate are summarized in Figure 3 where we plot the total mass of the argon gas Q crossing the counter's window (in gm/sec) vs. the total number of holes. This plot is equivalent to a plot of Q vs. K , as can be seen by the following reasoning.

The Knudsen number can be related to the number of holes as follows

$$N_{\text{holes}} D^2 = \frac{4}{\pi} A = \text{const} = \frac{4}{\pi} \cdot (10 \text{ cm}^2) \quad (2.48)$$

while the C-S parameter δ is given by

$$2\delta = \frac{D}{\lambda} = \frac{1}{K} \quad (2.49)$$

and therefore

$$N_{\text{holes}} = \frac{\text{const}}{D^2} = \frac{\text{const}}{A^2} \cdot K^2 = \text{const}' \cdot K^2 \quad (2.50)$$

for fixed value of the mean free path. The fluid analysis gives

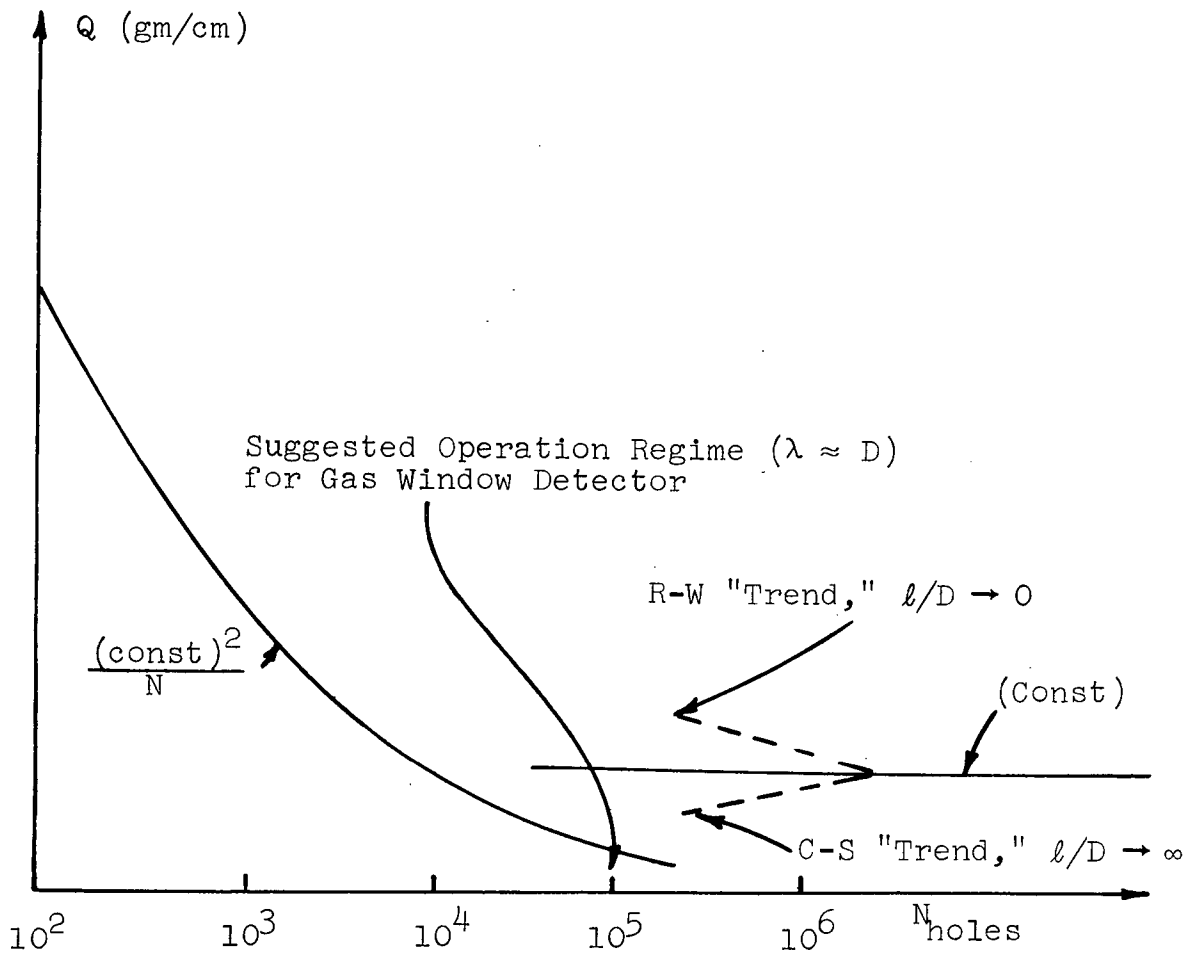


Figure 3. The Mass of Argon Gas Crossing the Counter's Window per Second as a Function of Number of Holes (with fixed total opened area). Indicated is the suggested regime for counter operation.

$$Q_{\text{const}} \propto N_{\text{holes}} D^4 = \frac{(\text{const})^2}{N_{\text{holes}}} \quad (2.51)$$

This behavior corresponds to small values of N_{holes} (left part of Fig. 3). The effusion value of Q is given by

$$Q_{\text{eff}} \propto N_{\text{holes}} D^2 = \text{const} \quad (2.52)$$

(right part of Fig. 3). Note that we are omitting two normalization constants in view of the uncertainties in the dependence on the geometric parameters and the accommodation coefficient. As the number of holes is raised, one can think of l fixed or as l/D fixed. In either case, the value of Q for $N_{\text{holes}} \rightarrow \infty$ is given by Kennard's formula. If l is fixed, the holes become long pipes as their number exceeds 10^5 , thus giving directional properties to the counter.

As it is clear from the figure, the trends suggested by the R-W and C-S calculations are not compatible but there is no actual contradiction since the parameters used in the two calculations and shown in Table 1 are not equivalent. We find from Kennard (Ref. 6, p. 308) that the value of the constant that gives Q for large N_{holes} satisfies

$$Q(l=a) \cong .7Q(l=0) \quad (2.53)$$

It is therefore likely that finite length l would offset the R-W "trend."

Even though it is unfeasible to determine purely theoretically the precise operation conditions without elaborate analysis, we reiterate that at least three additional factors can be utilized to minimize the argon flow: (1) proper shaping of holes, (2) proper choice of accommodating material for the porous window and (3) utilization of the helium-induced wall pressure and the thermal creep to counter the argon flow (e.g., by a suitable dependence of D on r).

III. HELIUM JET

We have considered several jet configurations. The design parameters illustrated in Figure 4 have desirable features. The idea is to use a high Mach number supersonic radial nozzle. The exit Mach number in Figure 4 is 7. The walls will be contoured such that the flow is parallel at the exit. The flow field of the jet has the following features.

The local Prandtl-Mayer expansion around the nozzle lip (point A) generates a leading characteristic surface (dashed line, C). Outside of this surface, the helium expands into a vacuum with a very large plume.

Between the characteristic surface and wall, the flow is essentially parallel but expands radially. (Note the top view in Fig. 4.)

A key point of the design is to choose the Mach number and exit height h_e sufficiently large that the surface C does not intersect the counter window. Then, the radial flow next to the window expands around the corner at B. A typical streamline is shown in Figure 4. This feature of the flow is most advantageous. The argon that is picked up by the helium jet is swept across the wall in a thin layer and expanded around the corner, hence, out of the field of x-ray view.

For the actual configuration shown in Figure 4, we now calculate the necessary flow properties. The flow near the wall (but not in the boundary layer) is a high Mach number radial isentropic expansion. From the known results for isentropic flow (e.g., see Ref. 11), we deduce the following approximations for the helium pressure and mass flux near the window:

$$\frac{p_w}{p_e} \approx \left(\frac{r_e}{r}\right)^{5/3}, \quad \frac{(\rho v)_w}{(\rho v)_e} \approx \frac{r_e}{r}, \quad r_e < r < r_c \quad (3.1)$$

where r is the radial distance from the center line, r_c is

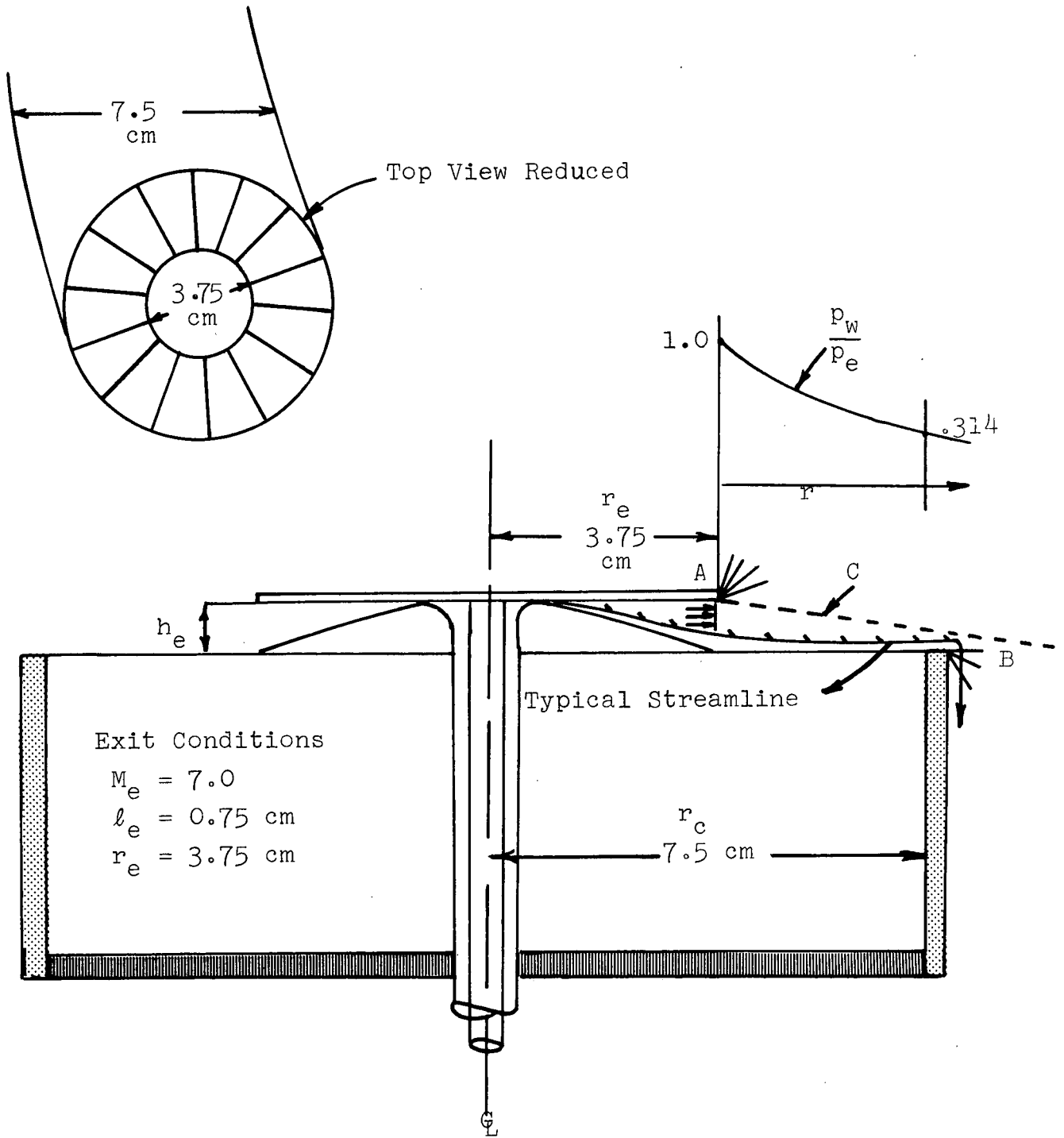


Figure 4. Helium Nozzle Geometry and Fluid Dynamic Properties with Suggested Parameter Values for Counter Operation. The lengths needed for design are:

- r_e = radius of helium jet exit surface
- r_c = radius of argon proportional chamber
- h_e = height of nozzle at exit

the outer edge of the window, and the subscripts e and w denote nozzle exit and counter window, respectively. The relations (3.1) are shown in Section IV to be valid in an isentropic, high Mach number flow (Eqs. (4.20) to (4.23)). The pressure along the counter window is plotted in Figure 4. The total drop across the window is about 50%.

The average pressure over the window is given by

$$\frac{\bar{p}_w}{p_e} = \frac{1}{A} \int_A \int \frac{p_w}{p_e} r \, dr \, d\theta \quad (3.2)$$

where $A = \pi(r_c^2 - r_e^2)$ is the total window area. Substitute for p_w/p_e from (3.1) to obtain

$$\frac{\bar{p}_w}{p_e} = 6 \left(\frac{\alpha^{1/3} - 1}{\alpha^2 - 1} \right), \quad \alpha = \frac{r_c}{r_e} \quad (3.3)$$

For $\alpha = 2.0$, we obtain $\bar{p}_w/p_e = 0.52$. Now, the average pressure on the window must be less than the chamber pressure. We choose $\bar{p}_w = 0.5$ mm Hg. Thus, the nozzle exit pressure must be 0.961 mm Hg. From the isentropic relation ($\gamma = 5/3$, Ref. 13, p. 313)

$$\frac{p}{p_t} = \left(1 + \frac{M^2}{3} \right)^{-5/2} \quad (3.4)$$

we obtain

$$\frac{p_e}{p_t} = 0.0087 \quad \text{at} \quad M_e = 7.0 \quad (3.5)$$

so that $p_t = 110$ mm Hg (helium supply pressure). We notice the important relation

$$p_t \propto p_e M_e^{-5} \quad (3.6)$$

that follows from (3.4) for the Mach number range of interest to us. The main freedom available in the design of the hypersonic nozzle is the exit Mach number M_e . The choice

$$M_e \sim 10 \quad (3.7)$$

would increase the helium flow rate by a factor of about 5 and thus decrease the blowing parameter by the same factor. Even under extreme effusion argon flow conditions, this helium jet would make the counter feasible. There is no theoretical limitation for the nozzle design; however, the small throat resulting may give rise to practical limitation on a smooth operation.

The throat area of the nozzle A^* is given by (Ref. 13, pp. 15-43 with $\Gamma = 5/3$)

$$\begin{aligned} \frac{A^*}{A_e} &= \frac{16}{9} M_e \left(1 + \frac{M_e^2}{3}\right)^{-2} \\ &= 0.0414 \text{ at } M_e = 7.0 \end{aligned} \quad (3.8)$$

For the configuration in Figure 3, the exit area is

$$\begin{aligned} A_e &= 2\pi r_e h_e \\ &= 17.65 \text{ cm}^2 \end{aligned} \quad (3.9)$$

Thus,

$$A^* = 0.73 \text{ cm}^2 \quad (3.10)$$

If we assume a throat radius $r^* = 1 \text{ cm}$, then the throat opening h^* can be calculated. We obtain

$$\begin{aligned} h^* &= \frac{A^*}{2\pi r^*} \\ &= 0.116 \text{ cm} \end{aligned} \quad (3.11)$$

(The helium mean free path is about $3 \times 10^{-4} \text{ cm}$; thus, fluid analysis holds.)

The helium mass flow rate is calculated from the relation

$$\begin{aligned} Q_{\text{He}} &= \rho^* A^* a^* \\ &= A^* \frac{\rho^*}{\rho_t} \frac{a^*}{a_t} p_t \sqrt{\frac{\gamma}{RT_t}} \end{aligned} \quad (3.12)$$

The density and velocity ratios are fixed by

$$\frac{\rho^*}{\rho_t} = \left(\frac{2}{\gamma + 1} \right)^{\frac{1}{\gamma - 1}} = 0.65 \quad (3.13)$$

$$\frac{a^*}{a_t} = \sqrt{\frac{2}{\gamma + 1}} = 0.866 \quad (3.14)$$

and we assume a total temperature $T_t = 300^\circ\text{K}$ ($R_{\text{He}} = 2.07 \times 10^7 \text{ cm}^2/\text{sec}^2\text{deg}$). Thus, we obtain the mass flow rate

$$Q_{\text{He}} = 0.985 \text{ gm/sec} \quad (3.15)$$

The throat Reynolds number is given by

$$\begin{aligned} \text{Re}^* &= \frac{\rho^* a^* h^*}{\mu^*} = \frac{Q_{\text{He}} h^*}{\mu^* A} \\ &\cong 1.0 \times 10^3 \end{aligned} \quad (3.16)$$

where we have used the viscosity of helium at the temperature T^* ($\mu^* = 1.59 \times 10^{-4}$, Ref. 2). Thus, we do not expect any dominant viscous effects for the nozzle. A Reynolds number based on conditions halfway between the nozzle exit and window edge is approximately 10^4 . Thus, the boundary layer thickness on the window can be expected to be less than 0.1 cm.

The mass flux at the exit is given by

$$\begin{aligned} \rho_e v_e &= Q_{\text{He}}/A_e \\ &= 0.056 \text{ gm/cm}^2/\text{sec} \end{aligned} \quad (3.17)$$

From (3.1), the flux decays as $1/r$ along the window. Thus, we have

$$0.056 > \rho_w v_w > 0.028 \quad (3.18)$$

The physical size of the window will be selected on the

basis of x-ray requirements. However, a diameter greater than 10 cm is desirable (but perhaps not necessary) for the nozzle design.

The helium nozzle design is determined by the window diameter, chamber pressure, and argon mass flow rate. First, the mass flow rate of the jet must be such that the blowing parameter is subcritical. The exit pressure, or at least the average wall pressure on the window, must be less than the chamber pressure. Finally, the jet Mach number and height of the jet are determined by the requirement that the leading characteristic surface does not impinge on the counter window. With the Mach number and size determined, the detailed nozzle geometry can be determined by the method of characteristics. The final design should be constructed and tested to ascertain the true wall pressure.

Since a higher value of the exit Mach number is needed if the argon flow is close to the effusion rate, we give, below, the relevant parameters for an exit Mach number that guarantees a subcritical blowing parameter (with the effusion value for the argon mass flow rate). Using Eqs. (3.4) and (3.12), we can write for the pressure in the helium tank

$$p'_t = \alpha p_t \quad (3.19)$$

and for the helium mass rate

$$Q'_{\text{He}} = \alpha Q_{\text{He}} \quad (3.20)$$

where

$$\alpha = \left[\left(1 + \frac{M_e'^2}{3} \right) / \left(1 + \frac{M_e^2}{3} \right) \right]^{5/2} \quad (3.21)$$

We then obtain the numerical values given in Table 2.

M_e	p_t	Q_{He}
7	110 mm Hg	.98 gm/sec
10	608 mm Hg	5.45 gm/sec
Table 2. Helium Jet Parameters		

We note that with the extreme value of the exit Mach number of 10, the pressure needed in the helium tank is

$$p_t(M_e=10) = 608 \text{ mm Hg} \cong .8 \text{ atm} \quad (3.22)$$

This value of the helium tank pressure is an upper bound that could be exceeded only if the R-W trend holds for the geometry used. (We use the conversion $1 A_s = 76 \text{ mm Hg} = 1.01 \times 10^6 \text{ dynes/cm}^2$.)

IV. HELIUM-ARGON INTERACTION

The final problem that we must consider is how the argon injection affects the helium flow. When fluid is injected into a boundary layer, there is a critical injection rate above which the boundary layer is "blown off" and the layer of injected substance thickens. This is undesirable in the present application since any argon outside of the window affects the x-ray measurement. We want to keep the argon in the boundary layer which we have estimated to be about 1 mm thick.

The so-called blowing parameter for flat plate boundary layer injection is defined by the formula (see Ref. 12)

$$b = \frac{2}{C_{f0}} \frac{(\rho v)_{Ar}}{(\rho v)_{He}} \quad (4.1)$$

where C_{f0} is a reference skin friction coefficient that is only a function of the Reynolds number. At the midpoint on the window, we have found that the Reynolds number is given by 10 .

$$Re \sim 10^4 \quad (4.2)$$

From Reference 12, page 38, Figure 49, we obtain

$$C_{f0} = 2.7 \times 10^{-3} \quad (4.3)$$

(This same value is obtained from Schlichting, Ref. 1, p. 286, Fig. 15.4.) The argon mass flux to be used in (4.1) is not the value given by Eq. (2.13) which is the flux at a particular hole. Rather, we take the total mass flow and divide it by the total window area. This latter is

$$\begin{aligned} A_w &= \pi(r_c^2 - r_e^2) \\ &= 133 \text{ cm}^2 \end{aligned} \quad (4.4)$$

Thus,

$$\begin{aligned}
 (\rho V)_{\text{Ar}} &= \frac{Q_{\text{Ar}}}{A_w} \\
 &= 0.00067 \text{ gm/cm}^2/\text{sec} \quad (4.5)
 \end{aligned}$$

From (4.1)

$$\begin{aligned}
 b &= \frac{2(.00067)}{(2.7 \times 10^{-3})(.056)} \\
 &= 8.85 \quad (4.6)
 \end{aligned}$$

The critical value of b is approximately

$$b_{\text{crit}} \sim 3 \quad (4.7)$$

(Reference 12 - The theoretical critical value of b , which is 4, is derived on page 69. The "practical" reduction of b_{crit} to 3 is discussed on page 70.) Thus, $b = 8.85$ is too large. The boundary layer would be blown off. We can reduce b , however, by reducing the argon flow rate. Reducing the porosity of the window is the most effective means of accomplishing this. From (4.1) we can calculate the critical argon flow rate.

$$\begin{aligned}
 (\rho v)_{\text{Ar}} &< b_{\text{cr}} \frac{C_{f0}}{2} (\rho v)_{\text{He}} \\
 &= 3 \frac{(2.7 \times 10^{-3})}{2} (.056) \\
 &= 2.27 \times 10^{-4} \text{ gm/cm}^2/\text{sec} \quad (4.8)
 \end{aligned}$$

This is about 1/4 of the value discussed in Section II. If we recall the D^4 dependence of the flow rate, only a very small change in D is needed.

We now use the effusion value (2.36) for the argon flow to calculate the blowing parameter. We have, using (2.34) and (2.36)

$$(\rho \bar{u})_{\text{eff}} \approx 2(\rho \bar{u})_{\text{cont}} \quad (4.9)$$

and, therefore, using (4.1)

$$b_{\text{eff}} \approx 2b_{\text{cont}} \approx 17.7 \quad (4.10)$$

This large value of the blowing parameter can be decreased by using a higher Mach number nozzle. First, we show that the skin friction coefficient is insensitive to Mach number. From Sandri, Kritz and Schatzman (Ref. 5, p. 490, Fig. 6), we see that the helium viscosity as a function of the temperature for the range of interest here is given by

$$\mu \propto T^{2/3} \quad (4.11)$$

From Schlichting (Ref. 1, p. 286, Fig. 15.4), we conclude (using (4.11) to set $\sigma(\text{Schlichting}) = 2/3$) that

$$C_{f,0} \sqrt{\text{Re}_{\text{He}}} = C_{f,0} \sqrt{\frac{u_{\text{He}} \ell \rho}{\mu}} \equiv F\left(\frac{2}{3}, M\right) \quad (4.12)$$

Figure 15.4 of Reference 1 is a plot of $F(\sigma, M)$. From Li and Lam (Ref. 13, p. 313), we find

$$T_e = T \left(1 + \frac{M^2}{3}\right) \quad (4.13)$$

Thus, for large Mach numbers,

$$T \propto M^{-2} \quad (4.14)$$

Using (3.6) for the Mach number dependence of the pressure, we find for the density

$$\rho \propto \frac{p}{T} \propto M^{-3} \quad (4.15)$$

From (4.12)

$$\begin{aligned}
c_{f,0} &\cong \left(\frac{\mu}{u_{\text{He}} \ell \rho} \right)^{1/2} F\left(\frac{2}{3}, M\right) \\
&\propto_F \cdot \left(\frac{\sqrt{T}}{M} \frac{1}{\rho} \right)^{1/2} \propto_F \cdot \left(\frac{M}{M} M^3 \right)^{1/2} \\
&\propto M^{3/2} \cdot F\left(\frac{2}{3}, M\right)
\end{aligned} \tag{4.16}$$

Therefore, we have the dependence of the skin friction coefficient on Mach number. The blowing parameter is now obtained as follows. From (4.16)

$$\begin{aligned}
\frac{c_{f,0}(M=10)}{c_{f,0}(M=7)} &= \frac{F\left(\frac{2}{3}, 10\right)}{F\left(\frac{2}{3}, 7\right)} \left(\frac{10}{7}\right)^{3/2} \\
&\cong 1.706 \times \frac{.85}{.90} = 1.6104
\end{aligned} \tag{4.17}$$

or

$$\begin{aligned}
c_{f,0}(M=10) &= 1.6104 \times (2.7 \times 10^{-3}) \\
&= 4.34 \times 10^{-3}
\end{aligned} \tag{4.18}$$

Thus, the skin friction coefficient is rather insensitive to Mach number in the range of interest. From Table 2, we find that

$$(\rho v)_{\text{He}}(M=10) = 5.55 (\rho v)_{\text{He}}(M=7) \tag{4.19}$$

Therefore, using Eq. (4.1)

$$b_{10} = .111785 \times b_7 \tag{4.20}$$

Therefore, using (4.10)

$$b_{\text{eff},10} = 1.98 < 3 \times b_{\text{ent}} \tag{4.21}$$

and thus we conclude that the helium boundary layer is not blown off.

We note that using the high Mach number isentropic relations (4.13), (4.15) (Ref. 13, p. 313) and the continuity equation for the helium jet

$$\rho v \cdot r = \rho_e v_e r_e \quad (4.22)$$

We find (remember that $v/\sqrt{T} \propto M$)

$$\frac{v}{\sqrt{T}} \propto \frac{1}{r \rho \sqrt{T}} \propto \frac{1}{r} M^4, \quad M \propto r^{1/3} \quad (4.23)$$

and

$$v \propto \frac{1}{r \rho} \propto \frac{M^3}{r} = \text{const} \quad (4.24)$$

Therefore

$$p \propto \rho^{+5/3} \propto (rv)^{-5/3} \propto r^{-5/3} \quad (4.25)$$

which coincides with Eq. (3.1).

V. CONCLUSIONS AND RECOMMENDATIONS

On the basis of our theoretical analysis, the gas window counter imposes design requirements that do not seem prohibitive. The most stringent of these is the high pressure in the helium tank. We believe that the upper value obtained in Section III, Eq. (3.22), is a very conservative bound since it is based on a pessimistic estimate of the argon flow rate. Since both the argon flow rate and the smooth functioning of the helium nozzle cannot be fully determined on theoretical grounds, we recommend that they be assessed with the help of experimental tests run in the parameter ranges indicated by the theoretical analysis.

We thank E. Boldt and P. Serlemitsos of the Goddard Space Flight Center for suggesting the problem and for useful discussions and P. Hu, R. Sullivan and J. Yates of Aeronautical Research Associates of Princeton, Inc. for useful discussions.

REFERENCES

1. Schlichting, H. Boundary Layer Theory, McGraw-Hill Pub. Co., N.Y., 1960.
2. Chapman, S. and Cowling, T.G. The Mathematical Theory of Nonuniform Gases, Cambridge University Press, 1960.
3. Yates, J. and Klimas, A. Aeronautical Research Associates of Princeton, Inc., Tech. Memo. 69-4, 1969.
4. Jeans, J. Introduction to Kinetic Theory of Gases, Cambridge University Press, pp. 44 and 163, 1946.
5. Sandri, G., Kritz, A.H. and Schatzman, F. Ann. Phys. (NY) 43, 452, 1967.
6. Kennard, E. Kinetic Theory of Gases, McGraw-Hill Pub. Co., N.Y., 1938.
7. Rotenberg, A. and Weitzner, H. "Nearly Free Flow through an Orifice," Phys. Fluids 12, 1573, 1969.
8. Sone, Y. and Yamamoto, K. "Flow of a Gas through a Circular Pipe," Phys. Fluids 11, 1672, 1968.
9. Cercignani, C. and Sernagiotto, F. "Cylindrical Poiseuille Flow of a Rarefied Gas," Phys. Fluids 9, 40, 1966.
10. Fujimoto, G. and Kato, S. "Rarefied Gas Flows through a Pipe Orifice," Rarefied Gas Dynamics Symp. No. 6, 1 (M. Trilling and H. Wachman, eds., Academic Press, N.Y., p. 685, 1959).
11. Equations, Tables and Charts for Compressible Flow, NACA Report 1135, 1953.
12. Kutateladze, S.S. and Leont'ev, A.I. Turbulent Boundary Layers in Compressible Gases, trans. by D.B. Spalding, Academic Press, N.Y., p. 24, 1964.
13. Li, W.H. and Lam, S.H. Principles of Fluid Mechanics, Addison-Wesley Pub. Co., 1964.
14. Zakkay, V., Calarese, W. and Sakell, L. "An Experimental Investigation of the Interaction of a Transverse Sonic Jet and a Hypersonic Stream," AIAA J. 9, 674, 1971.